INTERNATIONAL JOURNAL OF FOREST ENGINEERING, 2018
https://doi.org/10.1080/14942119.2018.1449444

Cutting performance comparison of low-kickback saw chain

Andrew Otto and John P. Parmigiani

School of Mechanical, Industrial, and Manufacturing Engineering, Oregon State University, Corvallis, OR, USA

ABSTRACT

Kickback is the leading cause of the most severe and traumatic chainsaw-related injuries. As a result, safety standards require chainsaw manufacturers to produce low-kickback saw chain. In order to understand the tradeoffs in current state-of-the-art saw chain, a comparison study was conducted on a custom test apparatus using four different saw chains, all with the same cutter geometry but different low-kickback chain features. Two modes of cutting were studied: nose-clear down bucking and boring. Cutting performance for boring with a chainsaw has not been studied previously. Regression modeling was used to generate cutting force and cutting efficiency trend lines for each of the different saw chains and cutting modes. In nose-clear down bucking, it was found that operator effort and cutting efficiency of a low-kickback chain with bumper drive links was of near-equal performance to that of a non-low-kickback chain (having no low-kickback features). In boring, all types of low-kickback saw chain elements required markedly higher operator effort and had lower cutting efficiency that of non-low-kickback saw chain. Furthermore, a substantial difference in cutting forces was found between differing designs of bumper drive link elements in both nose-clear down bucking and boring, highlighting the importance of proper bumper link geometry. Using these results and considering that the boring mode of operation is for experienced users, the casual chainsaw operator should always prioritize safety by using a low-kickback saw chain while professional users should select the chain that best suits their current cutting needs.

ARTICLE HISTORY
Received 21 November 2017
Accepted 5 March 2018

KEYWORDS
Chainsaw; saw chain; kickback; safety; regression

Introduction

Chainsaws are inherently dangerous to operate (Haynes et al. 1980; Koehler et al. 2004; Dąbrowski 2012; Hammig & Jones 2015). The most severe and traumatic chainsaw-related injuries – typically to the head and neck – are caused by chainsaw kickback (Brown 1995; Koehler et al. 2004; Dąbrowski 2012). Chainsaw kickback is the rapid motion of the guide bar towards the user (Koebke 1980; Roberson & Suggs 1991). The motion can be rotational or translational but the former is more common, more dangerous, and will exclusively be the focus of this paper. Rotational kickback occurs when the saw chain passing over the upper quadrant of the guide-bar tip (i.e. the end of the guide bar not attached to the chainsaw power head) contacts the workpiece, cuts too deeply, and comes to an abrupt stop (Koebke 1980; Roberson & Suggs 1991). Momentum is then transferred from the saw chain causing a rapid rotation, often exceeding 1000°/sec, of the guide bar towards the user (Arnold & Parmigiani 2015).

The danger associated with kickback has led to means for its prevention being included in the American National Standards Institute (ANSI) standard B175.1. This standard includes kickback-prevention design criteria that chainsaw manufacturers must satisfy. These criteria include a requirement that chainsaws have "features to reduce the risk of injury from kickback". The standard allows manufacturers some discretion in selection; however, features typically implemented on commercial chainsaws are reduced kickback guide bars, chain brakes, and low-kickback saw chain. Reduced kickback guide bars provide less area for kickback-inducing contact to occur by having specially-designed smaller-radius tips. Chain brakes quickly stop motion of the saw chain about the guide bar when kickback occurs, thus greatly reducing the potential for injury if contact with the operator occurs. Low-kickback saw chain inhibits overly deep cuts through modifications to cutter and link geometry.

Of these commonly-used means of reducing the risk of kickback, only low-kickback saw chain, due to limiting depth-of-cut, directly affects cutting effectiveness and efficiency. This has led to significant research and development efforts resulting in the commercial offering of many varieties of low-kickback saw chain designed to also cut well. These designs originated from patents describing special guard links in the saw chain to prevent jamming due to sticks and debris (Donley 1958; Carlton 1965). Adaptations of these guard links were then used to limit engagement of cutter teeth as they traversed the nose of the guide bar (Arff 1976; Goldblatt 1979; Olmr 1982). Through largely unpublished proprietary research, manufacturers continue to develop low-kickback saw chain to improve its cutting performance (Mang 2003; Goettel & Way 2011).

Evaluating the cutting performance of all types of saw chain is also a significant area of research, some of which has been published. Work with individual saw chain links has

CONTACT John P. Parmigiani John.Parmigiani@oregonstate.edu School of Mechanical, Industrial, and Manufacturing Engineering, Oregon State University, 204 Rogers Hall, Corvallis, OR 97331, USA

quantified the influence of cutter geometry and orientation on cutting forces (Gambrell & Byars 1966; Fujii et al. 1967; Stacke 1989). Instead of focusing on individual links, other research has used complete saw chains. McKenzie (1955) compared the performance of (at the time) newer saw chain designs to older "scratcher" type, while also developing useful metrics for evaluating the cutting performance of saw chain. Experiments by Reynolds (1970) revealed a linear relationship between cutting forces and depth-of-cut for saw chains. Stacke (1989) developed a full dynamic model for the saw chain during cutting using force data taken from single cutter experiments, and found similar linear relationships between depth-of-cut and cutting forces that was independent of chain velocity. Otto and Parmigiani (2015) used regression modeling to average the influence of wood physical properties on cutting force measurement, permitting comparison of chains across large numbers of wood specimens of the same species. Their work also showed that chains exhibit a peak cutting efficiency based on an overload depth-of-cut parameter.

Missing in the published literature is a scientific comparison of the cutting performance of low-kickback saw chain. To what extent is the performance of low-kickback saw chain reduced as compared to non-low-kickback saw chain (referred to hereafter as *professional saw chain*)? What tradeoffs exist when using a low-kickback saw chain? How do the various depth-of-cut limiting features used to create low-kickback saw chain affect cutting performance? This paper contributes to answering these questions by presenting a scientific study of the cutting performance of several modifications made to standard saw chain to create low-kickback saw chain. Specifically, this study compares four saw chains with identical cutting tooth geometries with different low-kickback elements. Data is generated using a custom saw-chain testing machine. Both nose-clear down-bucking (downward cuts not using the tip of the guide bar) and boring (plunge cuts using the tip of the guide bar) are included in the study. Results identify the differences in the performance of professional and low-kickback saw chains, as well as which cutting operations are most impacted by the use of a low-kickback saw chain.

Materials and methods

Saw chain

Saw chain can be classified as either professional or low-kickback. The key elements of a typical professional saw chain are illustrated in Figure 1(a) showing drive links, cutter links, and tie straps. Drive links engage a drive sprocket which propels the saw chain about the periphery of the guide bar. Cutter links consist of a chisel cutter and a depth gauge. The chisel cutter performs the actual wood cutting and the depth gauge limits its depth-of-cut. On professional chain, the depth gauge is the only feature that specifically controls depth-of-cut. The key elements of typical low-kickback saw chain are illustrated in Figure 1(b,c). The former shows a modified tie strap, referred to as a *bumper tie strap*, which is elevated and inclined to correspond to the depth gauge. Similarly, the latter shows a modified drive link, referred to as a *bumper drive link*, which also has an elevated and inclined section corresponding to the depth gauge. Both bumper tie straps and bumper drive links supplement the depth gauge in controlling depth-of-cut.

The need for supplemental control of depth-of-cut is illustrated in Figure 2 showing a section of professional chain

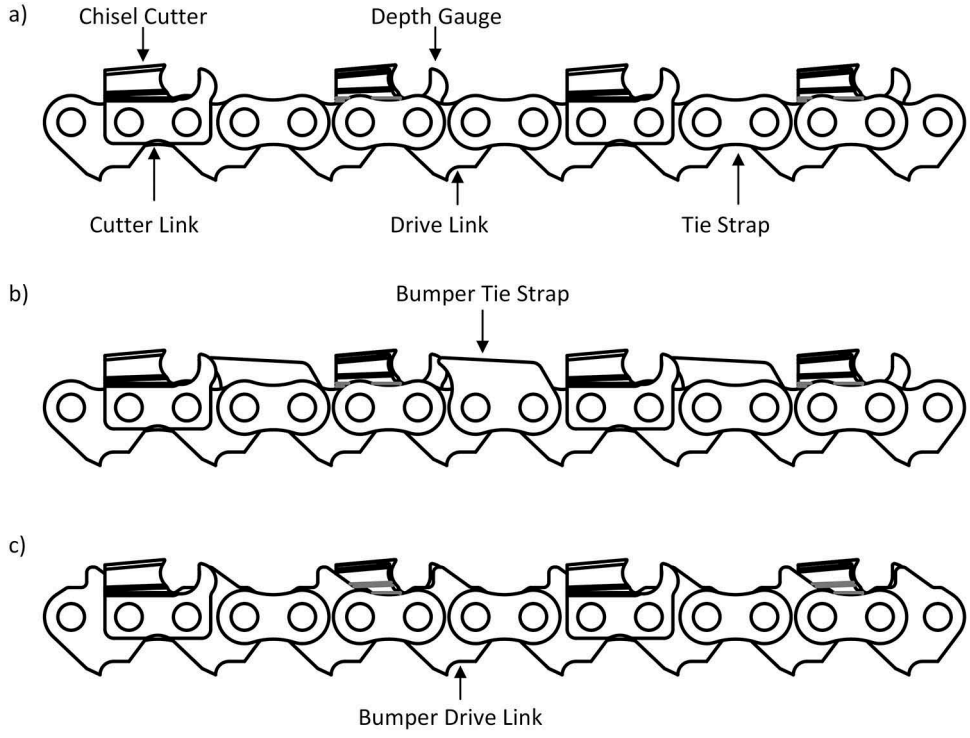

Figure 1. Typical saw chain components (a), low-kickback saw chain element bumper tie straps (b), and low-kickback saw chain element bumper drive link (c).

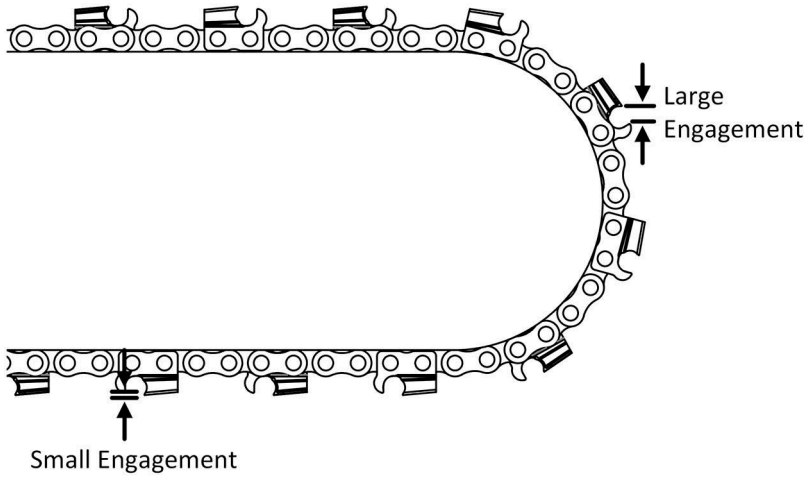

Figure 2. Increase in depth-of-cut as cutter links traverse the guide bar nose is a cause of kickback.

traversing the free end of a guide bar. Note the large difference in the depth-of-cut allowed by the depth gauge for a (down) bucking cut versus a boring cut. When the saw chain is traversing the upper or lower surfaces of the guide bar, as during bucking cutting, the chain links are aligned and the depth gauge is effective in limiting the depth-of-cut of the cutter link to relatively small values. However, when the saw chain is traversing the nose of the guide bar, as during boring or other cutting involving the bar tip, the links are not aligned and the depth gauge is much less effective and allows a large depth-of-cut which can lead to chainsaw kickback. Bumper tie straps and bumper drive links are specifically designed to limit depth-of-cut when the saw chain is traversing the nose of the guide bar by articulating relative to the cutter link.

Four saw chains were selected for this study. All four chains had the same cutter link geometry. The only difference between each chain was the low-kickback feature present. Each chain was in the new, out-of-box condition. The first chain, denoted *Chain A*, was professional chain and contained no low-kickback features and is thus referred to as the *naked specimen*. The second, denoted as *Chain B*, featured bumper tie straps meeting the ANSI B175.1 standard and is referred to as the *bumper tie strap specimen*. The third and fourth, denoted to as *Chain C* and *Chain D*, respectively, both contain bumper drive links. Chain C and Chain D have a slight difference in the geometry of their bumper drive links and are included in the study to highlight the influence of chain-link geometry on cutting performance. Specifically, Chain C has a larger ramped portion on the top of the drive link compared to Chain D. They are referred to respectively as the *Bumper Drive Link – 1 specimen* and the *Bumper Drive Link – 2 specimen*. The same guide bar and six-tooth spur sprocket were used for all chains throughout testing.

Measured and calculated parameters

The same measured cutting parameters used in previous work (Otto & Parmigiani 2015) are adapted for the current work, along with the boring cutting mode of operation. Classically, cutting experiments with saw chain have been performed in the nose-clear down bucking mode, where the guide bar is fed vertically downward into a workpiece with the nose of the guide bar being clear of material. In this work, testing is also conducted in the boring mode of operation, where the nose of the guide bar is plunged horizontally into the workpiece and fed until the nose exits the opposite side of the workpiece. In nose-clear down bucking, the cutting force (F_C) and feed force (F_F) are the measured reaction forces on the workpiece in the horizontal and vertical directions, respectively. This convention is reversed for boring, as displayed in Figure 3, where cutting force is the reaction force in the vertical direction and feed force is the reaction force in the horizontal direction. The saw chain is propelled by the drive sprocket with drive torque T_M and angular velocity ω. The reaction force on the bar due to chain tension is denoted F_T. The feed

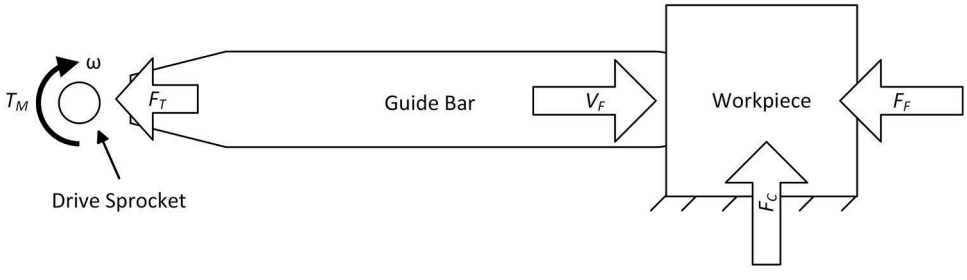

Figure 3. A diagram of a chainsaw performing a boring cut showing the measured cutting parameters of drive torque (T_M) and velocity (ω), chain tension (F_T), feed force (F_F) and velocity (V_F), and cutting force (F_C).

velocity is denoted V_F, which is always in the direction of the feed force and the motion of the body of the saw.

Three quantities are calculated from the parameters defined in Figure 3, with equations listed in Table 1. The chain force (F_{CH}) is the effective tangential force applied by the motor torque to drive the chain through the wood during cutting. Here the variable n is the number of teeth on the derive sprocket. Chain velocity (V_C) is the speed of the chain as it moves around the periphery of the bar and is a function of the drive sprocket velocity. Depth-of-cut is the theoretical chip thickness cut by each pair of left- and right-handed cutter pairs and depends upon chain velocity, feed velocity, chain pitch (P), and tooth spacing (S) (Otto & Parmigiani 2015).

Test apparatus

The test apparatus used in this work was developed previously (Otto & Parmigiani 2015) and accurately measures the parameters described above under rate-controlled conditions. The apparatus uses standard off-the-shelf guide bars and drive sprockets. Three subsystems make up the mechanical portion of the machine: the power head, which drives the chain with an AC motor; the work holding system, which measures reaction forces and restrains the workpiece; and the motion system, which has two linear axes of motion and controls the cutting rate. An overall view of the machine, with labeled subsystems, is shown in Figure 4. Motor drive torque (T_M), chain tension (F_T), cutting force (F_C), and feed force (F_F) are recorded during cutting at 2 kS/s using industry standard strain-gage based torque and force transducers and a National Instruments CompactRIO data acquisition system running LabVIEW. A 200-point moving average filter was used to reduce mechanical noise present in the measured torque and force waveforms.

Table 1. Calculated cutting parameters as functions of sprocket drive torque (T_M), chain pitch (P), number of sprocket teeth (n), sprocket angular velocity (ω), feed velocity (V_F), and tooth spacing (S).

Parameter	Calculation	
Chain force (N)	$F_{CH} = T_M\left(\frac{\pi}{(1000P)n}\right)$	(1)
Chain velocity (m/s)	$V_C = \frac{\omega}{2\pi}2(1000P)n$	(2)
Depth-of-cut (mm)	$\delta = \frac{V_F}{V_C}P\ S$	(3)

Test media

Workpieces for testing were obtained from Douglas-fir dimensional timbers 3.0 m in length with rectangular cross section (90 × 140 mm). They were hand-selected from a local lumber supplier such that the grain was oriented vertically in nose-clear down bucking and horizontally in boring to allow the chain to instantaneously pass through equal amounts of early- and late-wood while cutting. The end-grain orientations for each mode are displayed in Figure 5. The number of knots was minimal. Each timber was divided into four 25-cm long workpieces, sized to fit in the safety enclosure of the testing machine. Cuts were equally spaced in each workpiece to produce offcuts of approximately 20 mm in thickness.

Test procedure

Each cut performed with the test apparatus followed the same procedure, which is similar to that used in previous testing with the same machine (Otto & Parmigiani 2015). First, the guide bar and one of the four chains for testing were installed on the power head. Then, the workpiece corresponding to the current randomized experimental run was inserted into the work holding system. Next, the power head was turned on at

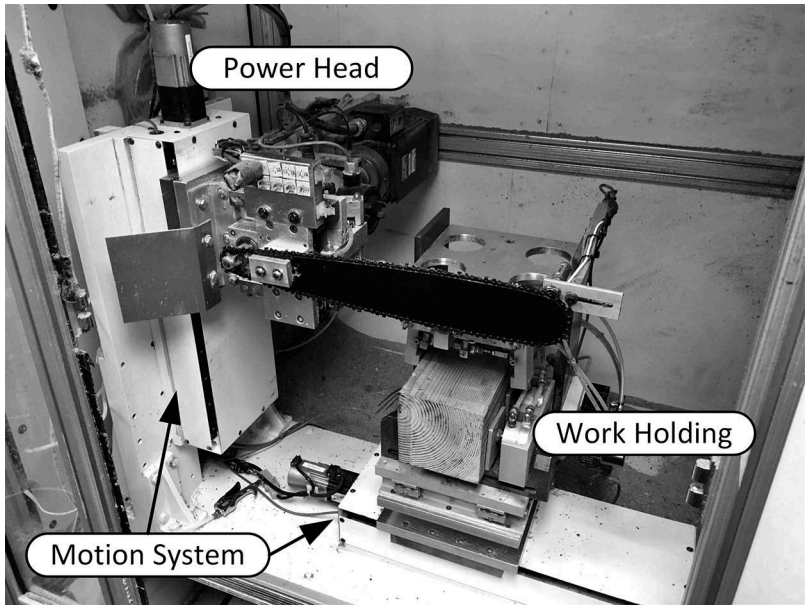

Figure 4. Image of the testing machine used to measure cutting forces and control cutting rates during experiments showing the three subsystems.

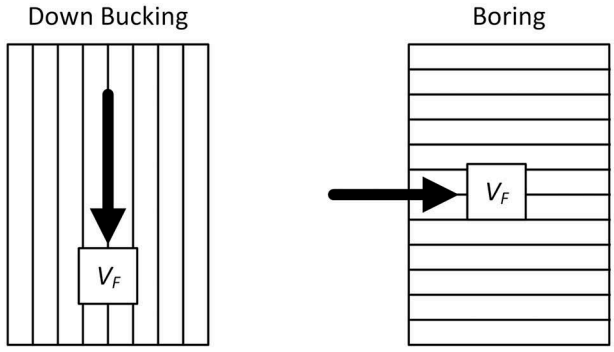

Figure 5. End-grain orientations for down bucking and boring cutting modes.

the desired chain speed to take an average measurement of the non-cutting chain tension for two seconds. If the chain tension was above or below the specified control point for any test by more than 5 N, the machine would request adjustment by the operator. Adjustment, if necessary, was performed using the tensioner screw located on the bar mount of the power head. Once the chain tension was within tolerance, the machine would again start the power head at the desired chain velocity, dwell for 1 second, weigh the workpiece, and perform the cut at the desired feed rate while recording force and torque values. Following the cut, the machine would return to its starting position and automatically load the chain velocity and feed rate for the next cut, awaiting operator input to start the next cut. All cuts were performed with bar lubricating oil applied at a manufacturer recommended 5 mL/min through the standard oiling orifice of the guide bar.

Immediately after cutting, each offcut was collected for measurement of moisture content and density. Moisture content was measured using a Delmhorst J-200 moisture content meter by inserting the measuring probes into the center of the wood cross section. Density was calculated from the measured mass and volume of the offcut. Mass was measured with a gram scale and offcut volume (length × width × height) was measured using digital machinist's calipers.

Data processing

Several post processing steps were necessary before using the collected data for regression modeling, and are largely identical to those used in earlier work with the same experimental setup (Otto & Parmigiani 2015). First, the raw torque and force values were passed through a 200-point moving average filter to remove noise. Workpiece weight was subtracted from the measured vertical reaction force during cutting. Motor drive torque was converted into chain force (F_{CH}). These steps result in the cutting force waveforms shown in Figure 6(a). For regression modeling, a singular measured value is required from each cut that represents the cutting force. To achieve this, an effective average is obtained by placing each force channel into 15 equally spaced bins of a histogram, and picking the center point of the bin with the highest frequency of samples as the representative force value, which is displayed in

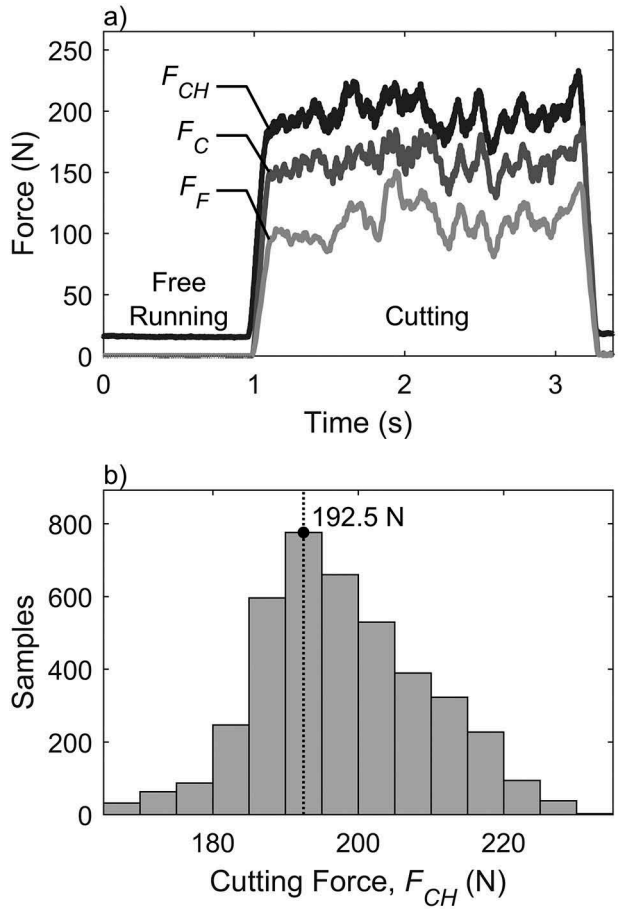

Figure 6. (a) Representative cutting force waveform collected during a single cut, (b) the histogram method used to extract the effective cutting force (192.5 N in this case) from the force waveforms.

Figure 6(b). Past work has shown this method to be effective in reducing the influence of knotty samples on skewing cutting data, allowing the inclusion of cuts with knots present in the regression model (Otto & Parmigiani 2015).

Data analysis

Multiple linear regression was used for analyzing the raw cutting data and generating trends for each test. The measured chain force, cutting force, and feed force served as responses for linear regression. Three predictors were used: the controlled variable depth-of-cut (specified) and the uncontrolled variables moisture content and density (measured). Prior work has shown that tracking workpiece properties allows for reduction of the influence wood heterogeneity has on the cutting force data (Otto & Parmigiani 2015). Furthermore, including workpiece properties in the regression models permits comparisons between different chain designs even though the separate tests did not all cut in the exact same test media. Chain velocity was held fixed at 7.62 m/s (4000 RPM on a 6-tooth sprocket) for all testing, as prior work has shown cutting velocity has little effect on cutting forces in the velocity envelope of the testing machine, which is approximately 1500–7000 RPM (Otto & Parmigiani 2015).

The regression model used has all main effects as well as the interactions of moisture content and density with depth-of-cut. This model was selected based on its adequacy in preceding tests with similar chains and test media (Otto & Parmigiani 2015), with the only difference being the omission of chain velocity as a predictor variable. The model equation used for down bucking is of the form:

$$F_{CH}, F_C, F_F = \beta_0 + \beta_1(MC^*) + \beta_2(\rho^*) + \beta_3(\delta^*) + \beta_4\delta - \delta_{OL} + \beta_5(MC^*)(\delta^*) + \beta_6(\rho^*)(\delta^*),$$

where:

$$\langle \delta - \delta_{OL} \rangle = \begin{cases} 0 \text{ if } \delta^* \le \delta_{OL} - \bar{\delta} \\ \delta - \delta_{OL} \text{ if } \delta^* > \delta_{OL} - \bar{\delta}. \end{cases}$$

In the preceding, MC refers to moisture content, ρ is wood density, δ is the depth-of-cut, and δ_{OL} is the overload depth-of-cut, as defined by Otto and Parmigiani (2015), and is used for bilinear regression in depth-of-cut. Overload depth-of-cut is the depth-of-cut value at which the bilinear response between force and depth-of-cut changes to have a different constant of proportionality (i.e. slope). Variables with an asterisk superscript (i.e. MC^*) have been centered about their mean value for samples within that particular subset of chain's data. For example, $\rho^* = \rho - \bar{\rho}$, where the overbar notation denotes the mean value of a given predictor variable for one of the four chains.

The model equation used for boring cuts is of the form:

$$F_{CH}, F_C, F_F = \beta_0 + \beta_1(MC^*) + \beta_2(\rho^*) + \beta_3(\delta^*) + \beta_4(MC^*)(\delta^*) + \beta_5(\rho^*)(\delta^*)$$

where the only difference from down bucking is the omission of the overload depth-of-cut term (δ_{OL}), as large depths of cut are generally not attainable in the boring cutting mode.

Results

Collected data and regression model

Testing consisted of making repeated cuts with each chain at varying depths of cut and fixed chain speed (7.62 m/s). Seven depth-of-cut levels (0.05, 0.15, 0.25, 0.35, 0.45, 0.55 and 0.65 mm) were used for each chain in the down bucking cutting mode, while five levels (0.05, 0.0875, 0.125, 0.1625, and 0.2 mm) for each chain were used in the boring cutting mode. Eight replicates of each depth-of-cut level for each of the four saw chains resulted with a total of 224 cuts (56 cuts for each chain) in down bucking and 160 cuts (40 cuts for each chain) in boring. These cuts were dispersed between the workpieces, with four replicates in each workpiece. Cuts were randomized within workpieces to reduce systematic error.

Before forming the regression models, the raw data for the workpiece properties of moisture content and density was studied. Average values and standard deviations of workpiece properties with respect to each chain tested are displayed in Table 2. Overall, moisture content varied from 10.1% to 26.8% and density from 452 to 733 kg/m^3. The large range in density is attributed to the few offcuts with knots present. Low moisture content levels were only present in a small number of cuts that occurred near the open ends of the timbers due to air drying during storage at room temperature. Within each cutting mode, the distribution of wood material properties was consistent across each chain, which enables cross-comparison of the regression model results when the physical properties are treated as random variables.

Table 2. Measured workpiece moisture content and density.

		Moisture content (MC) (%)		Density ρ (kg m^{-3})	
Cutting mode	Chain	Mean	Standard deviation	Mean	Standard deviation
Down bucking	A	23.9	2.8	491	24.6
	B	24.7	0.6	498	27.4
	C	24.8	0.6	531	62.6
	D	24.9	0.6	512	54.9
	Total	24.6	1.6	508	46.6
Boring	A	23.6	2.1	555	24.9
	B	21.0	3.7	537	47.2
	C	23.6	2.4	547	18.7
	D	23.7	1.5	548	23.6
	Total	22.8	3.0	547	31.1

Regression coefficients and model fitment summary, quantified by the coefficient of determination (R^2) and F-statistic, are provided in Table 3 for the down bucking experiment and in Table 4 for the boring experiment. Overall, good fit was obtained as indicated by high R^2 values and statistically significant regression with F-values much greater than the critical F-value for the experiments ($F_{6,49,0.05}$ = 2.29 for down bucking and $F_{5,34,0.05}$ = 2.49 for boring). Lower R^2 values were

Table 3. Regression model coefficients and fit for chain force (F_{CH}), cutting force (F_C), and feed force (F_F), down bucking.

		Regression coefficients							Fit	
Chain		β_0	β_1	β_2	β_3	β_4	β_5	β_6	R^2	F
A	F_{CH}	103.36	−0.91	0.02	239.83	84.54	−3.01	0.46	0.99	690
	F_C	80.92	−0.82	−0.09	224.72	50.33	−4.21	0.01	0.98	339
	F_F	31.73	−0.05	−0.05	90.97	104.82	0.87	−0.16	0.98	407
B	F_{CH}	108.93	−3.54	0.03	256.14	75.51	−16.89	−0.26	0.99	880
	F_C	79.39	1.31	−0.03	227.93	63.71	−10.03	−0.12	0.99	1080
	F_F	37.69	1.71	−0.01	120.09	198.16	−4.08	−0.12	0.99	574
C	F_{CH}	106.18	7.15	0.13	272.53	84.59	16.68	0.40	0.99	766
	F_C	78.24	8.59	0.12	228.40	114.95	16.74	0.47	0.99	565
	F_F	41.84	6.33	0.08	138.86	215.30	30.34	0.26	0.96	168
D	F_{CH}	105.40	2.33	0.10	247.48	32.77	7.04	0.17	0.99	782
	F_C	77.42	1.60	0.08	212.82	43.50	−3.32	0.13	0.99	712
	F_F	31.63	4.96	−0.01	89.53	99.18	23.77	−0.09	0.98	320

Table 4. Regression model coefficients and fit for chain force (F_{CH}), cutting force (F_C), and feed force (F_F), boring.

		Regression coefficients						Fit	
Chain		β_0	β_1	β_2	β_3	β_4	β_5	R^2	F
A	F_{CH}	82.46	−1.62	0.14	239.77	−4.98	1.14	0.95	123
	F_C	79.61	−0.20	0.02	120.05	6.05	0.58	0.75	21
	F_F	41.58	−1.14	0.07	106.46	−5.77	0.41	0.90	60
B	F_{CH}	93.81	−1.29	0.12	290.69	−4.04	0.57	0.95	128
	F_C	108.40	−1.24	0.05	273.07	−3.54	1.61	0.84	36
	F_F	57.30	−1.97	0.20	160.49	−6.85	0.85	0.87	45
C	F_{CH}	95.78	−3.43	0.23	276.00	−11.91	1.84	0.87	38
	F_C	119.43	−2.70	0.24	303.37	16.10	3.53	0.85	32
	F_F	46.77	−2.64	0.18	146.09	−18.86	0.30	0.85	31
D	F_{CH}	85.77	−1.42	0.17	249.91	−5.70	1.51	0.97	221
	F_C	89.69	1.52	0.17	164.03	−0.02	0.94	0.87	44
	F_F	39.27	−2.60	0.04	122.53	−5.47	0.23	0.93	89

obtained for the boring cutting experiment which is attributed to covering a smaller range in depth-of-cut compared to the down bucking experiment.

For down bucking, each chain required different values of the overload depth-of-cut for the regression models shown in Table 5. The overload depth-of-cut values used in the regressions were selected by forming the root mean square error (RMSE) of feed force as a function of overload depth-of-cut, which is displayed in Figure 7. Feed force was used over the other responses as it proved most sensitive to this fitting parameter. Minimizing the RMSE of feed force as a function of overload depth-of-cut enabled objective selection of an overload depth-of-cut value that accurately captures the bilinear-overload behavior of saw chain, as shown in related work (Otto & Parmigiani 2015), provided a global minimum exists.

Regressions for feed force were formed for 100 linearly spaced overload depth-of-cut values between 0.1 and 0.6 mm to generate the RMSE versus overload depth-of-cut function in Figure 7. Resultant minimums and their respective feed force RMSE values are reported in Figure 6. As can be seen, all chains' feed force RMSE displayed a definite, unique minimum. Chain D had the lowest overload depth-of-cut at 0.29 mm while Chain B had the highest at 0.49 mm. Chains A and C had very similar overload depth-of-cut values of 0.39 mm and 0.38 mm, respectively. Chain C had the largest feed force RMSE of 9.34 N, while the other three chains were all grouped in the 4–5 N zone.

Cutting forces and cutting efficiency comparison

Using the regression coefficients in Tables 3 and 4, trend lines were calculated for chain force, cutting force, and feed force vs. depth-of-cut for both the down bucking and boring modes. A fourth group of trend lines was formed by calculating the cutting efficiency (η) from chain force, as defined by Otto and Parmigiani (2015), and plotting vs. depth-of-cut. All trend lines are shown in Figure 8. The influence of moisture content and density was factored out of the trend lines by using the total averages for both moisture content and density listed in Table 3 for down bucking and boring.

For down bucking, the four chains performed similarly in respect to chain force, cutting force, and cutting efficiency as indicated by the tight proximity of the trend lines and peak values in Figure 8. Feed force (F_F) showed the largest differences between chains. The peak feed force values for Chains A-D were 85, 104, 137 and 90 N, respectively. The "knee" in each of the trend lines is due to the presence of the overload depth-of-cut parameter in the regression model for down bucking.

In boring, straight line fits were obtained for each force trend line vs. depth-of-cut due to the absence of the overload depth-of-cut parameter from the regression model. The chain force (F_{CH}) trend lines are largely parallel, with Chain A (naked) exhibiting the lowest peak chain force of 100 N and Chain C (bumper drive links) having the highest peak chain force of 122 N. Again, feed force had the largest differences between chains with peak values of 88, 128, 145, and 100 N for Chains A-D, respectively. In cutting efficiency, Chain A was the best performer with a peak of 1.96 mm^2/J, while Chain C had the lowest efficiency with a peak of 1.61 mm^2/J. Overall, Figure 8 clearly shows that the Chain A had the lowest cutting forces as well as the highest efficiency in the boring cutting mode. Furthermore, Chain D (bumper drive links) closely follows the cutting performance of Chain A while meeting the ANSI low-kickback standard.

Table 5. Selected overload depth-of-cut values, down bucking.

Chain	Overload depth-of-cut δ_{OL} (mm)	Feed force F_F RMSE (N)
A	0.39	4.30
B	0.49	4.18
C	0.38	9.34
D	0.29	5.15

RMSE, root mean square error.

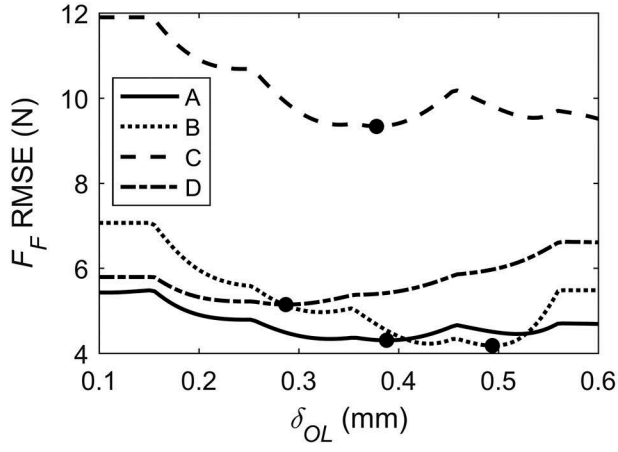

Figure 7. Root mean square error (RMSE) of feed force (F_F) as a function of overload depth of cut (δ_{OL}) for each chain used in the low-kickback study in down bucking. Minimums are indicated using solid dots on each line.

Discussion

The similarity in forces for down bucking in the cutting direction (F_{CH} and F_C) between chains in Figure 8(a,b) is attributed to each chain having the same cutter link geometry. This similarity in forces is expected since the different low-kickback elements primarily work in the direction that opposes the feed direction of the chain (perpendicular to the cutting direction), hence having minimal effect on the cutting forces. On the other hand, differences in feed force among chains for down bucking (Figure 8(c)) as well as all forces for boring (Figure 8[e–h]) are attributed to the different low-kickback elements between each chain working in opposition of the feed direction.

Ideally, a saw chain cuts with the least force input from the operator. In other words, a high-performing saw chain should cut with large depth of cut under typical feed forces. Thus, a high-performing saw chain would cut with greater speed than a lower-performing chain under the same feed force input from the operator. Typical feed forces in down bucking are close to the weight of the saw itself, which is roughly 50 N. Inspecting Figure 8(c) and reading the depth-of-cut for each chain at 50 N ranks the chains in terms of cutting speed, with the best-to worst ranking for down bucking being Chain A-B-D-C. Interestingly, the y-intercepts on the feed force plot for

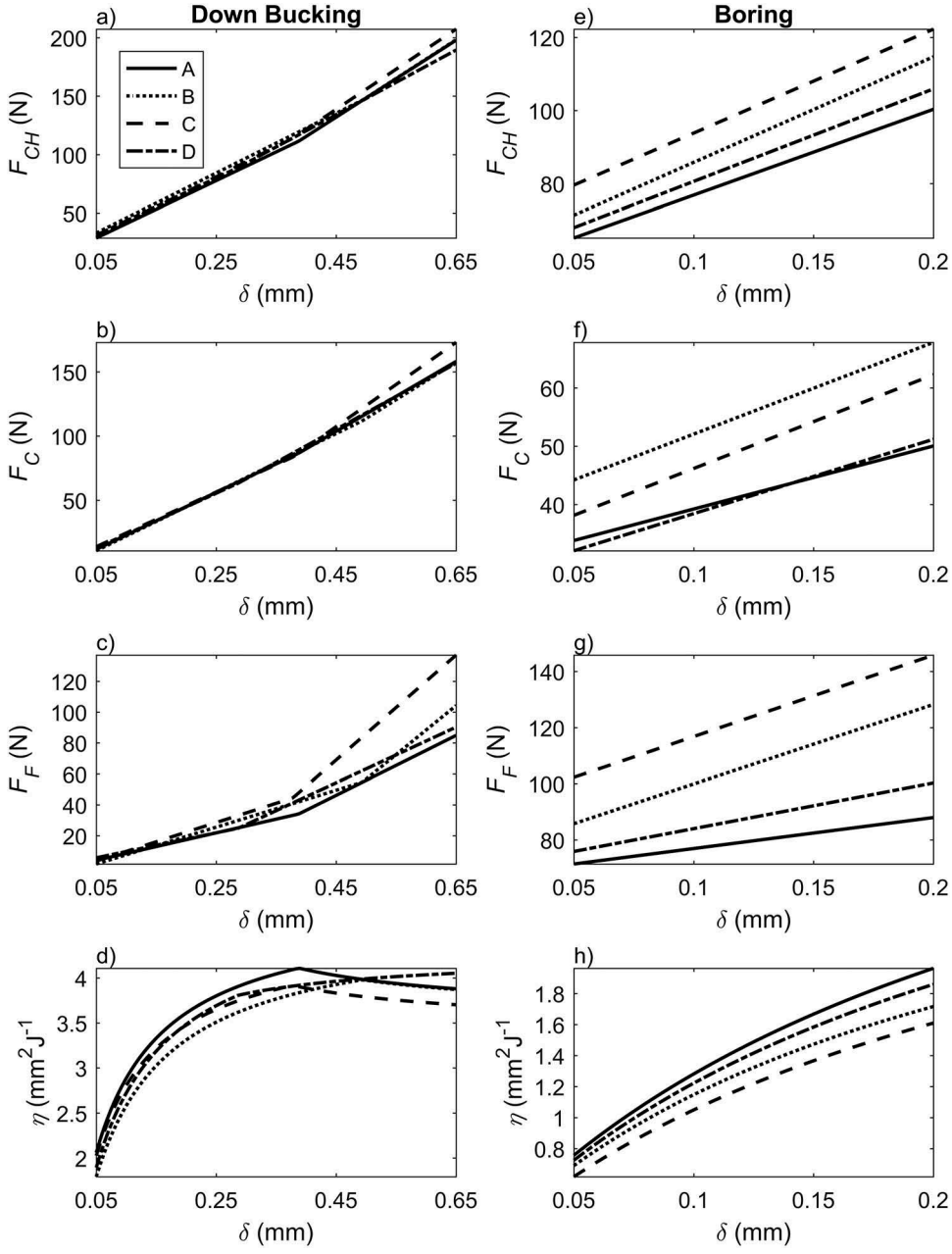

Figure 8. Chain force (F_{CH}), cutting force (F_C), feed force (F_F), and cutting efficiency (η) plotted versus depth of cut (δ) for each of the four chains (A, B, C, D) used in the low-kickback comparison study for both the down bucking (left column, a–d) and boring (right column, e–h) cutting modes.

down bucking of Figure 8(c) are nearly identical across all four chains, which indicates the slope of the trend line controls the cutting rate along with the "knee" in the trend line due to the overload depth-of-cut. Therefore, feed force vs. depth-of-cut slope (N/mm) and overload depth-of-cut (mm) are useful descriptors of the cutting performance for a chain in the down bucking cutting mode. In the boring cutting mode, the performance differences between chains can be clearly seen from the feed force in Figure 8(g). The best-to-worst ranking in terms of boring feed force is Chain A-D-B-C.

Another interesting result from the experiment comes from comparing Chain C and Chain D (bumper drive links). The only feature separating these chains is a slight difference in the bumper drive link shape. Despite this small difference, the variation in cutting forces between these two chains is considerable in both down bucking and boring. Chain C was the overall worst-performing low-kickback saw chain while Chain D was the overall best performing. The large performance difference highlights the sensitivity of low-kickback link geometry to cutting forces and the importance of careful low-kickback link design.

In the general case, cutting performance differences between a *properly designed* low-kickback saw chain and the non-low-kickback version are small under *most* operating conditions. Therefore, the present experimental results support the notion that saw chain meeting the ANSI B175.1 low-kickback saw chain standard should be used

for the large majority of chainsaw operations for improved safety. Certainly, low-kickback saw chain will not perform boring cuts as easily as a non-low-kickback saw chain since that is precisely the type of cutting the bumper links act to prevent. It is the intent of the authors that this study provides useful quantitative information on the performance differences between low-kickback and professional saw chain such that consumers and professionals alike can always prioritize safety depending on the type of cutting being performed.

Conclusions

The cutting performance of three low-kickback saw chains and one professional saw chain was compared under controlled cutting conditions in down-bucking and boring cutting modes. Under all cutting conditions, professional saw chain exhibited the lowest cutting forces and therefore the highest cutting efficiencies. For typical depth-of-cut values, the performance advantage of a professional saw chain in down bucking was marginal compared to the best-performing low-kickback saw chain, which used bumper drive links. Feed force, an indicator of operator effort during cutting, was the most sensitive response to changes in low-kickback saw chain elements. Large differences in feed force between the professional chain and low-kickback chains were observed in the boring cutting mode. Additionally, each chain required different overload depth-of-cut values in the regression model despite having the same cutter link geometry, indicating the safety elements control depth-of-cut and the onset of overload during cutting. Therefore, overload depth-of-cut can serve as a useful parameter for comparing different chains.

The data presented for testing in the boring cutting mode under controlled conditions is new to the chainsaw cutting literature. In addition, this study provides a method for determining a saw chain's overload depth-of-cut using regression methods. For general use, the authors recommend low-kickback rated saw chain for two reasons: (1) chainsaws are most commonly operated in nose-clear down bucking conditions, and (2) the measured cutting performance differences in this study are small under down bucking conditions.

The results of this study highlight the sensitivity of cutting performance to the geometry of the low-kickback links on saw chain. Investigation into the influence of low-kickback link geometry on cutting performance would be a useful extension of the present work. One of the main challenges in low-kickback link design is parameterizing the shape in such a way to enable controlled design iteration – essentially establishing the dependence of cutting forces on link shape.

Disclosure statement

No potential conflict of interest was reported by the authors.

References

Arff UF, Outboard Marine Corporation, assignee. 1976 Apr 20. Saw chain. Patent US3951027 A.

Arnold D, Parmigiani JP. 2015. A study of chainsaw kickback. For Prod J. 65:232–238.

Brown ATF. 1995. Chainsaw penetrating neck injury. J Accid Emerg Med. 12:134–137.

Carlton RR, Omark Industries Inc., assignee. 1965 Apr 27. Brush cutting chain. Patent US3180378 A.

Dąbrowski A. 2012. Reducing kickback of portable combustion chain saws and related injury risks: laboratory tests and deductions. Int J Occup Saf Ergon. 18:399–417.

Donley RW, RW Donley, assignee. 1958 Mar 11. Cutter chain for power saws. Patent US2826226 A.

Fujii Y, Sugihara H, Suzuka M. 1967. Study on wood cutting ability of single chain-saw tooth. II. J Jpn For Soc. 49:1–8.

Gambrell SC Jr, Byars EF. 1966. Cutting characteristics of chain saw teeth. For Prod J. 16:62–71.

Goettel M, Way A, Blount Inc., assignee. 2011 Aug 30. Saw chain drive link with tail. Patent US8006598 B2.

Goldblatt L, Jessie Goldblatt, assignee. 1979 Jan 9. Kickback-free saw chain. Patent US4133239 A.

Hammig B, Jones C. 2015. Epidemiology of chain saw related injuries, United States: 2009 through 2013. Adv Emerg Med. 1–4. doi:10.1155/2015/459697

Haynes CD, Webb WA, Fenno CR. 1980. Chain saw injuries: review of 300 cases. J Trauma. 20:772–776.

Koebke RH. 1980. Chainsaw kickback dynamics. J Mech Des. 102:247–248.

Koehler SA, Luckasevic TM, Rozin L, Shakir A, Ladham S, Omalu B, Dominick J, Wecht CH. 2004. Death by chainsaw: fatal kickback injuries to the neck. J Forensic Sci. 49:1–6.

Mang H, Andreas Stihl Ag & Co. Kg, assignee. 2003 Oct 16. Saw chain. Patent US20030192418 A1.

McKenzie WM. 1955. Performance of gouge type power saw chains. Aust Timber J. 21:938–954; 995.

Olmr JJ, Textron Inc., assignee. 1982 Sept 14. Safety saw chain. Patent US4348927 A.

Otto A, Parmigiani JP. 2015. Velocity, depth-of-cut, and physical property effects on saw chain cutting. BioResources. 10:7273–7291.

Reynolds DD, Soedel W, Eckelman C. 1970. Cutting characteristics and power requirements of chain saws. For Prod J. 20:28–34.

Roberson GT, Suggs CW. 1991. Construction and evaluation of a chainsaw kickback simulator. Appl Eng Agric. 7:153–157.

Stacke LE. 1989. Cutting action of saw chains [Ph.D. dissertation]. Gothenburg: Chalmers University of Technology.